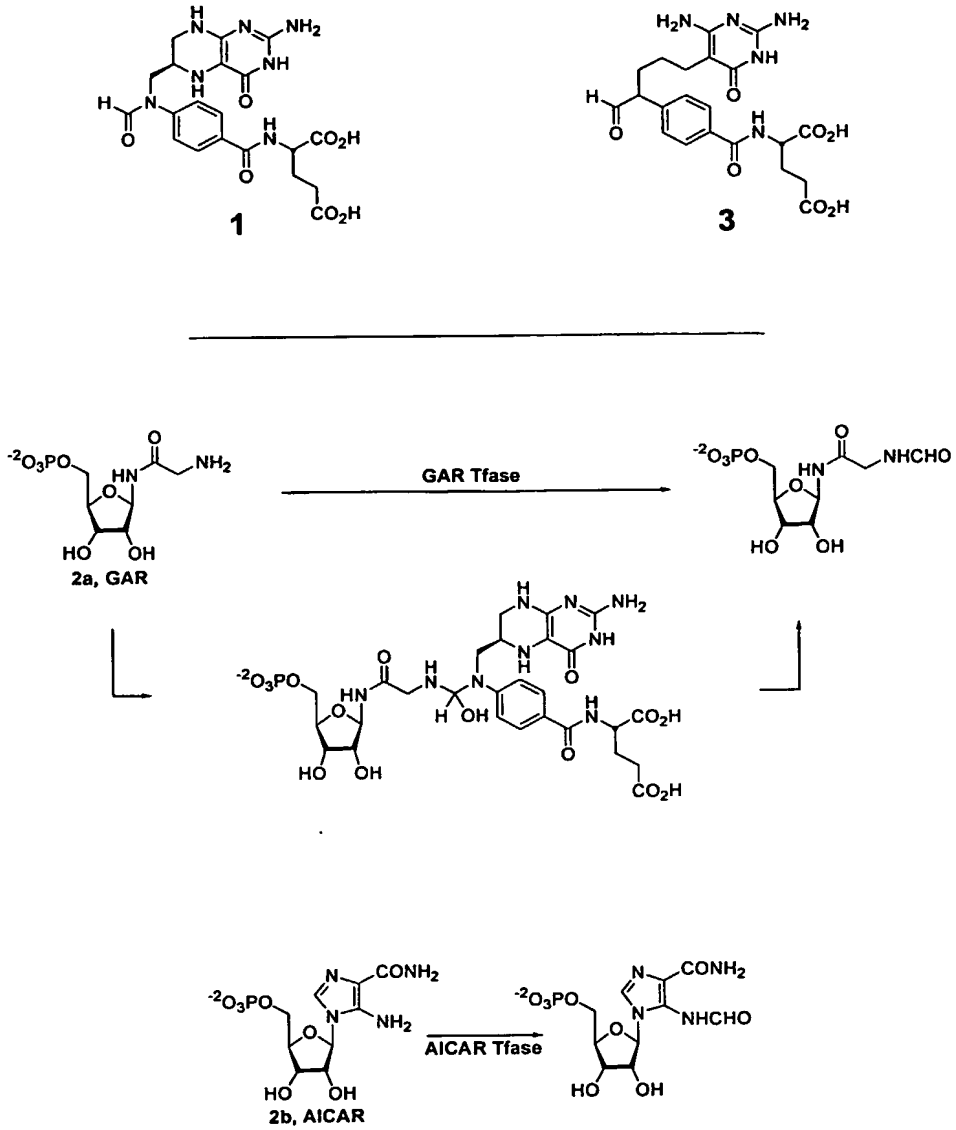

Figure 1

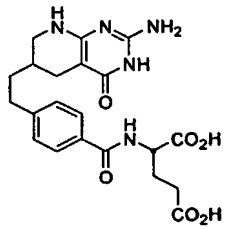

4, DDATHF

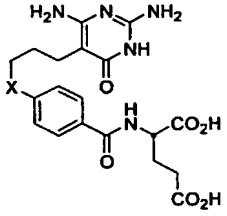

5, X = CH_2, NH, S

Figure 2

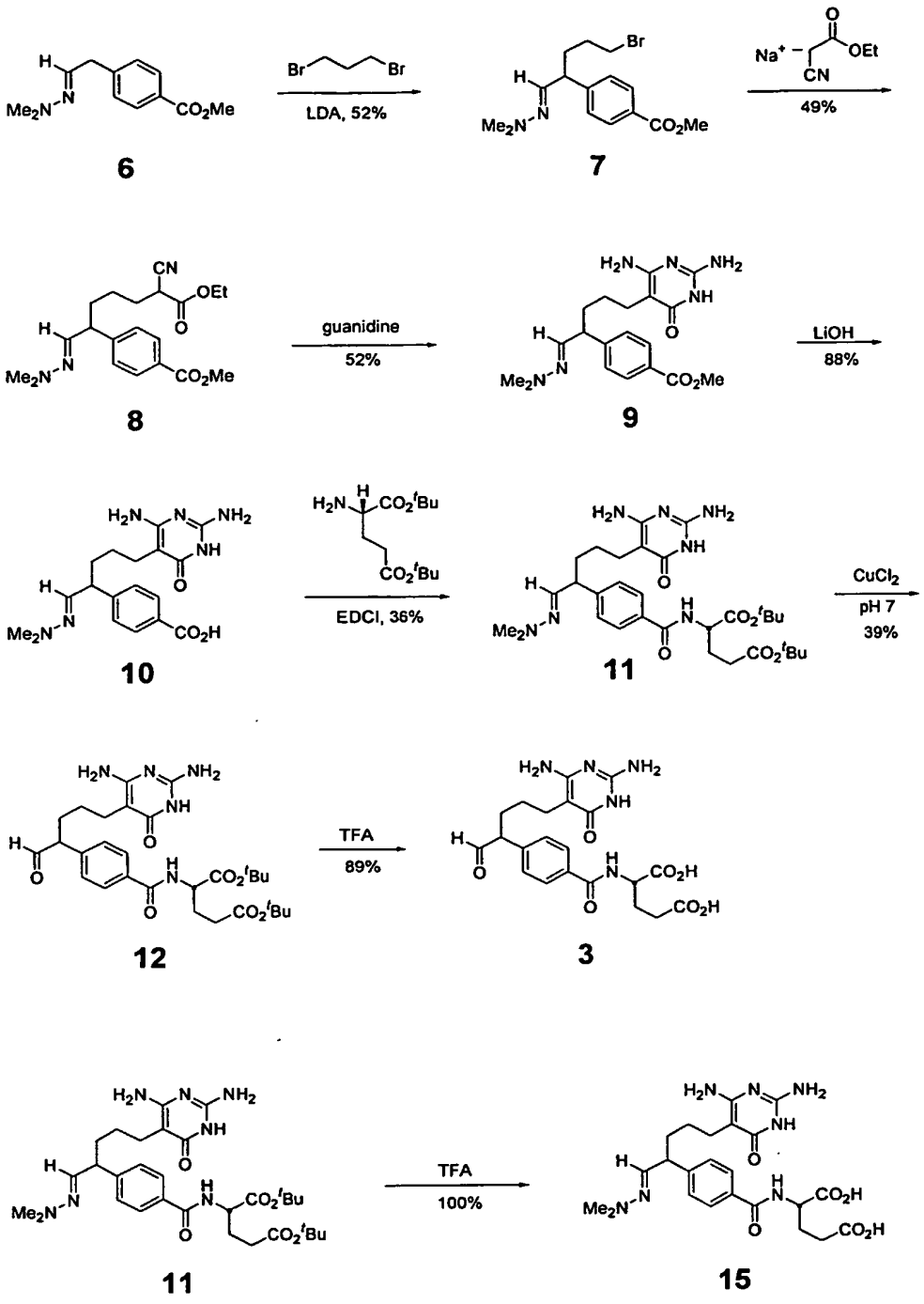
Br Br
LDA, 52%
Na+ − O OEt CN
49%
guanidine
52%
LiOH
88%
EDCI, 36%
CuCl2
pH 7
39%
TFA
89%
TFA
100%
6
7
8
9
10
11
12
3
11
15

Figure 3

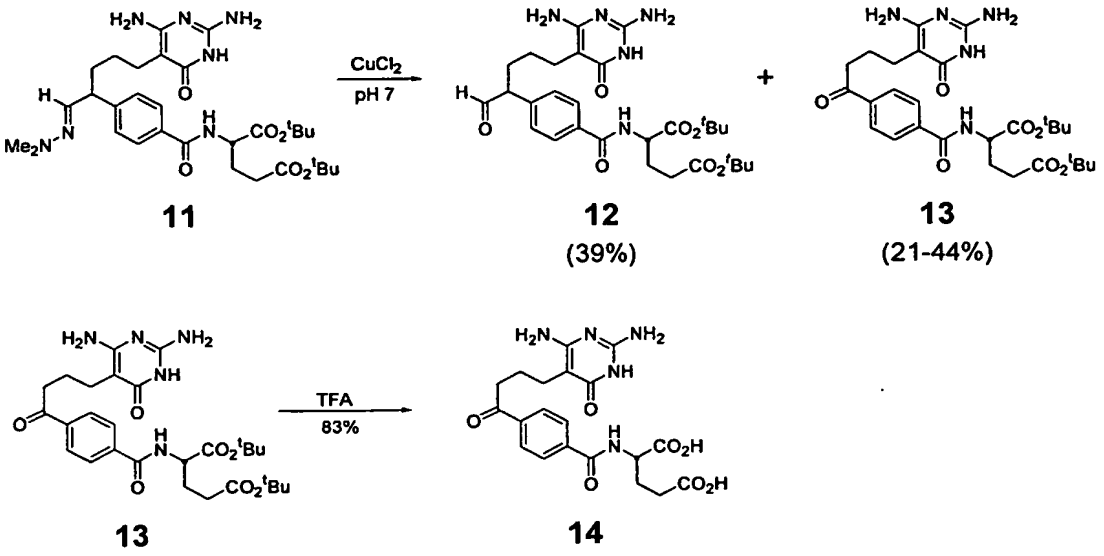

Figure 4

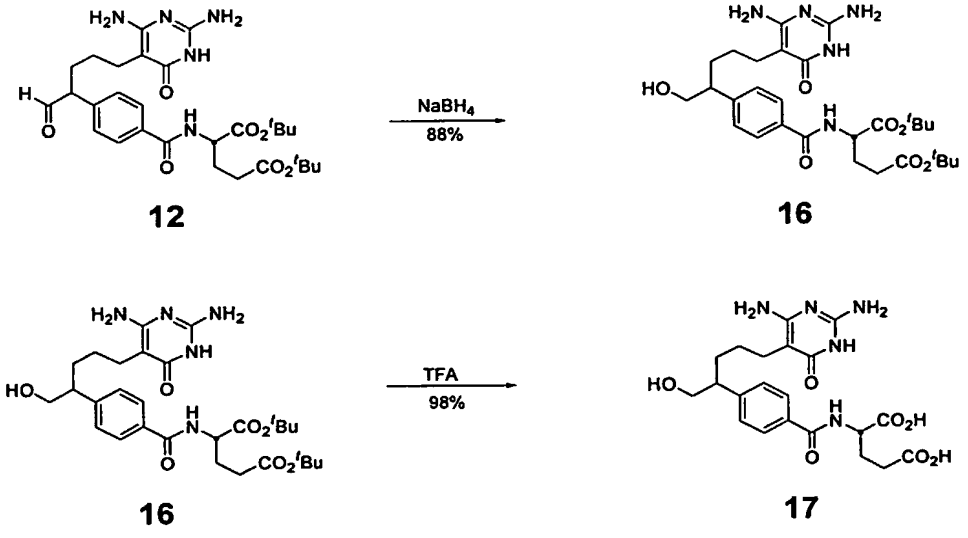

Figure 5

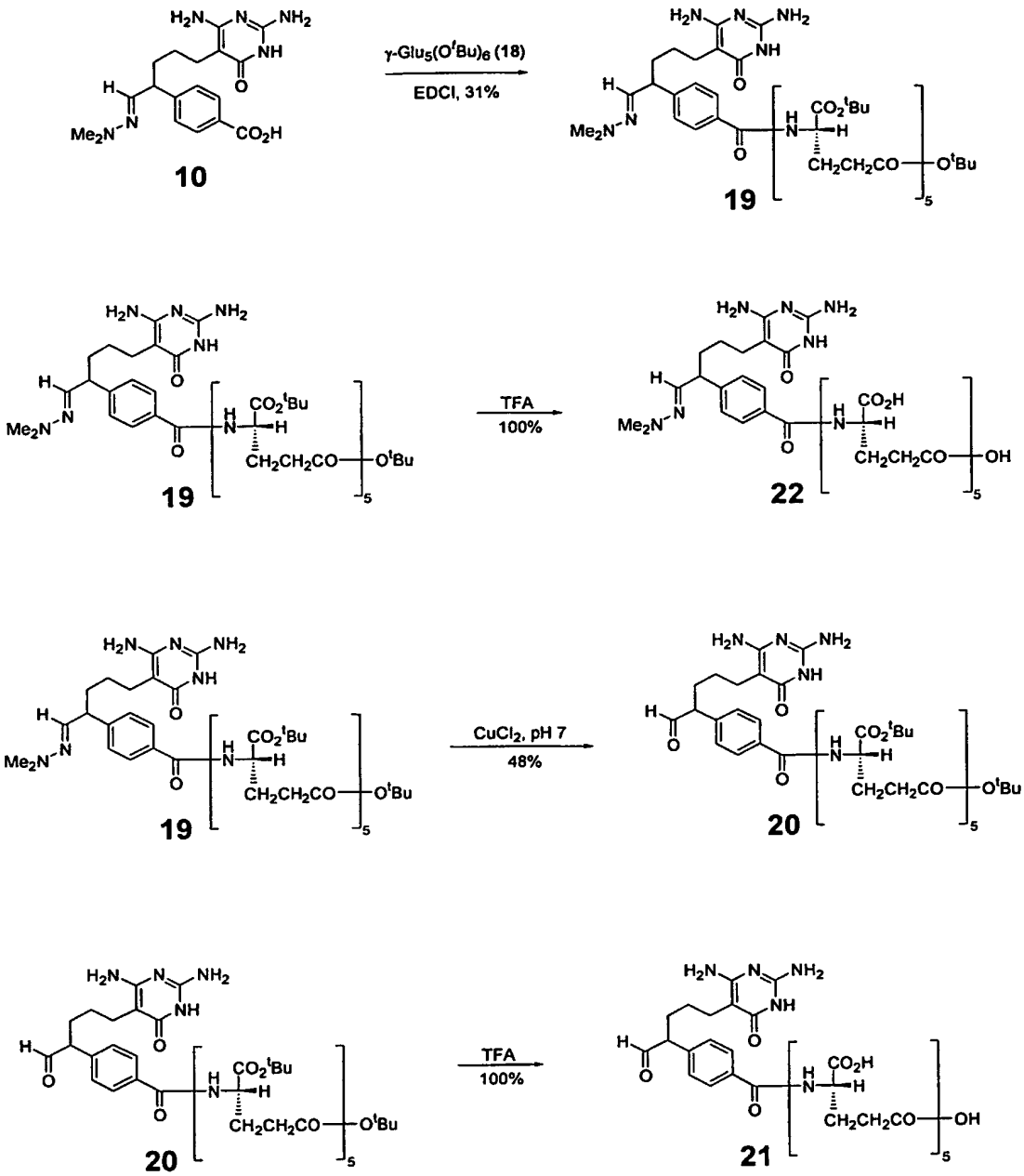

Figure 6

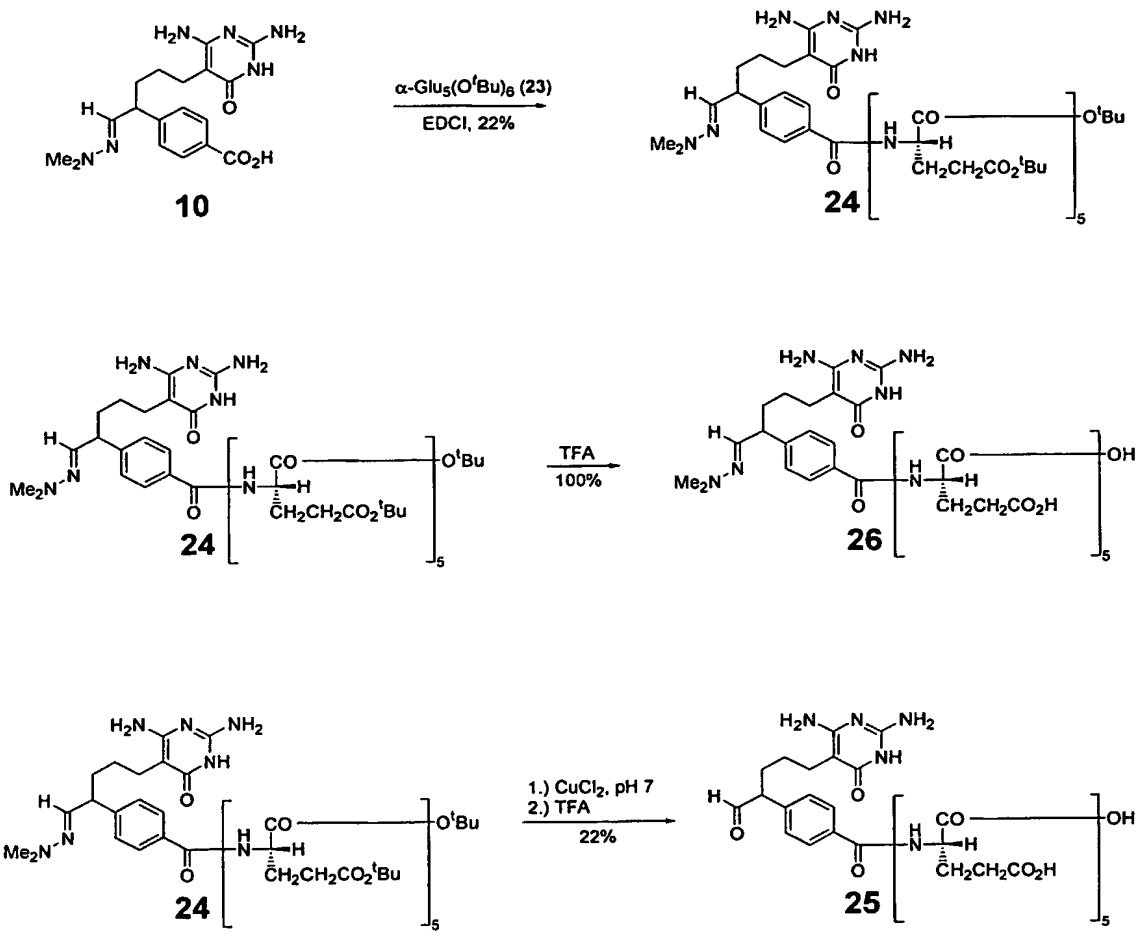

Figure 7

GAR Tfase, AICAR Tfase, and DHFR inhibition (K_i, μM)[a]

compound	K_i GAR Tfase	K_i AICAR Tfase	K_i DHFR
9	17	>100	>100
10	48	>100	>100
11	>100	>100	>100
12	5	1	>100
3	6	1	>100
14	24	>100	>100
15	6	28	>100
17	16	>100	>100
21	2.7	0.26	25
22	1.9	0.20	62
25	16	16	>200
26	23	7.1	>200
Lometrexol	0.1	nd[b]	nd[b]

[a] *E. coli* GAR Tfase, human AICAR Tfase, and *E. coli* DHFR
[b] nd, not done

Figure 8

In Vitro Cytotoxic Activity

	CCRF-CEM (IC_{50}, μM)			
compound	(+) T, (+) H[a]	(–) T, (+) H	(+) T, (–) H	(–) T, (–) H
9	225	>250	80	90
10	>250	>250	>250	>250
11	50	50	50	40
12	50	50	40	50
3	150	170	0.06	0.07
14	80	80	0.20	0.10
15	>200	>200	0.04	0.03
17	>200	160	0.04	0.03
21	>100	>100	>100	>100
22	>100	>100	>100	>100
25	80	60	9	7
26	>100	>100	7	6
Lometrexol	>250	>250	0.20	0.15

[a]T = Thymidine, H = Hypoxanthine

Figure 9

In Vitro Cytotoxic Activity in the Presence of AICAR

	CCRF-CEM (IC_{50}, μM)			
compound	(–) T, (–) H, (–) A[a]	(+) T, (–) H, (–) A	(–) T, (+) H, (–) A	(–) T, (–) H, (+) A
3	0.07	0.06	>150	>150
14	0.10	0.20	>200	>200
15	0.03	0.04	>200	>200
17	0.03	0.04	>200	>200
Lometrexol	0.15	0.20	>200	>200

[a]T = Thymidine, H = Hypoxanthine, A = AICAR monophosphate

Figure 10

In Vitro Cytotoxic Activity

	CCRF-CEM/MTX (IC_{50}, μM)			
compound	(+) T, (+) H[a]	(–) T, (+) H	(+) T, (–) H	(–) T, (–) H
3	130	>200	140	>200
14	>100	nd	nd	>100
15	>200	>200	>200	>200
17	>100	nd	nd	>100
Lometrexol	>200	>200	>200	>200
	CCRF-CEM/FPGS$^-$ (IC_{50}, μM)			
compound	(+) T, (+) H[a]	(–) T, (+) H	(+) T, (–) H	(–) T, (–) H
3	>100	nd	nd	>100
14	>100	nd	nd	>100
15	>100	nd	nd	>100
17	25	nd	nd	55
Lometrexol	>100	nd	nd	>100

[a]T = Thymidine, H = Hypoxanthine

Figure 11

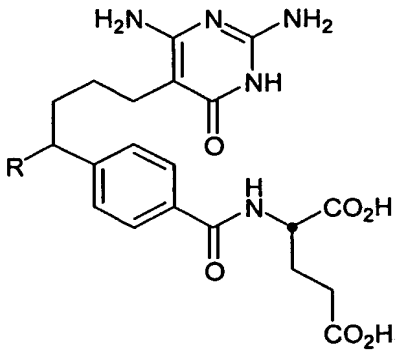

E. coli and rhGAR Tfase inhibition (K_i, μM).

compound	K_i *E. coli* GAR Tfase	K_i rhGAR Tfase
3 R = CHO	6	0.014
14 R = O=	24	13
15 R = $CH{=}NNMe_2$	6	0.17
17 R = CH_2OH	16	1.7
21 (γGlu_5-**3**)	2.7	0.013
22 (γGlu_5-**15**)	1.9	0.032
25 (αGlu_5-**3**)	16	0.034
26 (αGlu_5-**15**)	23	0.12
Lometrexol	0.1	nd

Figure 12

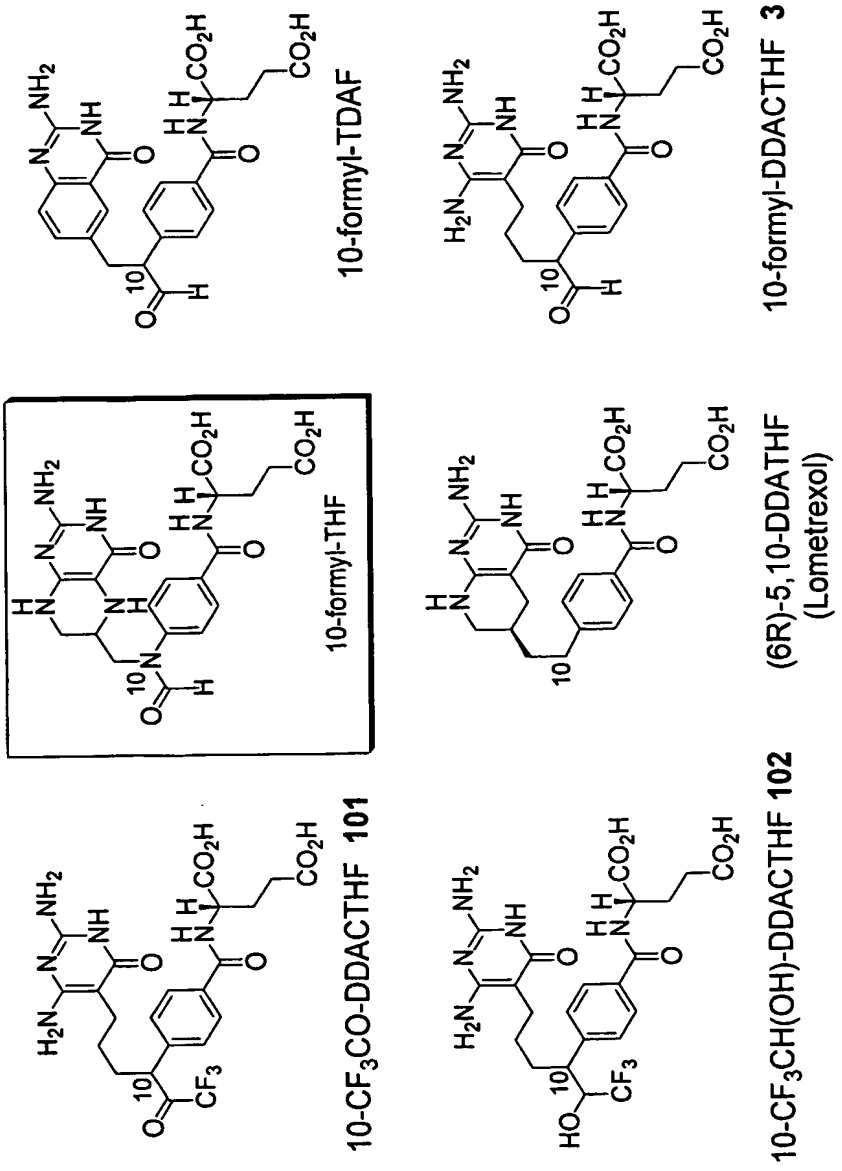
10-formyl-TDAF
10-formyl-THF
10-formyl-DDACTHF 3
10-CF3CO-DDACTHF 101
(6R)-5,10-DDATHF
(Lometrexol)
10-CF3CH(OH)-DDACTHF 102

Figure 13

Data Reduction	
spacegroup	$P3_121$
unit cell	a = b = 126.24 Å, c = 94.42 Å
no. of molecules per a.u.	2
resolution (Å)	45-1.98 (2.01-1.98)[1]
completeness (%)	99.7 (100)
multiplicity	3.9 (3.8)
average I/σ	24.9 (2.0)
[2]R_{sym} (%)	7.4 (60.1)
Refinement	
data cutoff	$F_o > 0\sigma$
reflections (test set)	57912 (2913)
protein atoms	3016
water molecules	251
inhibitor atoms	76
average protein B value (Å^2)	33.1
average inhibitor B value (Å^2)	32.5
average solvent B value (Å^2)	36.8
RMSD from ideal	
bond length (Å)	0.014
bond angle (deg)	1.37
[3]R_{cryst} (%)	22.7
[4]R_{cryst} (%)	24.7
Ramachandran plot (%)	
most favored	92.6
Additionally allowed	7.4

Figure 14

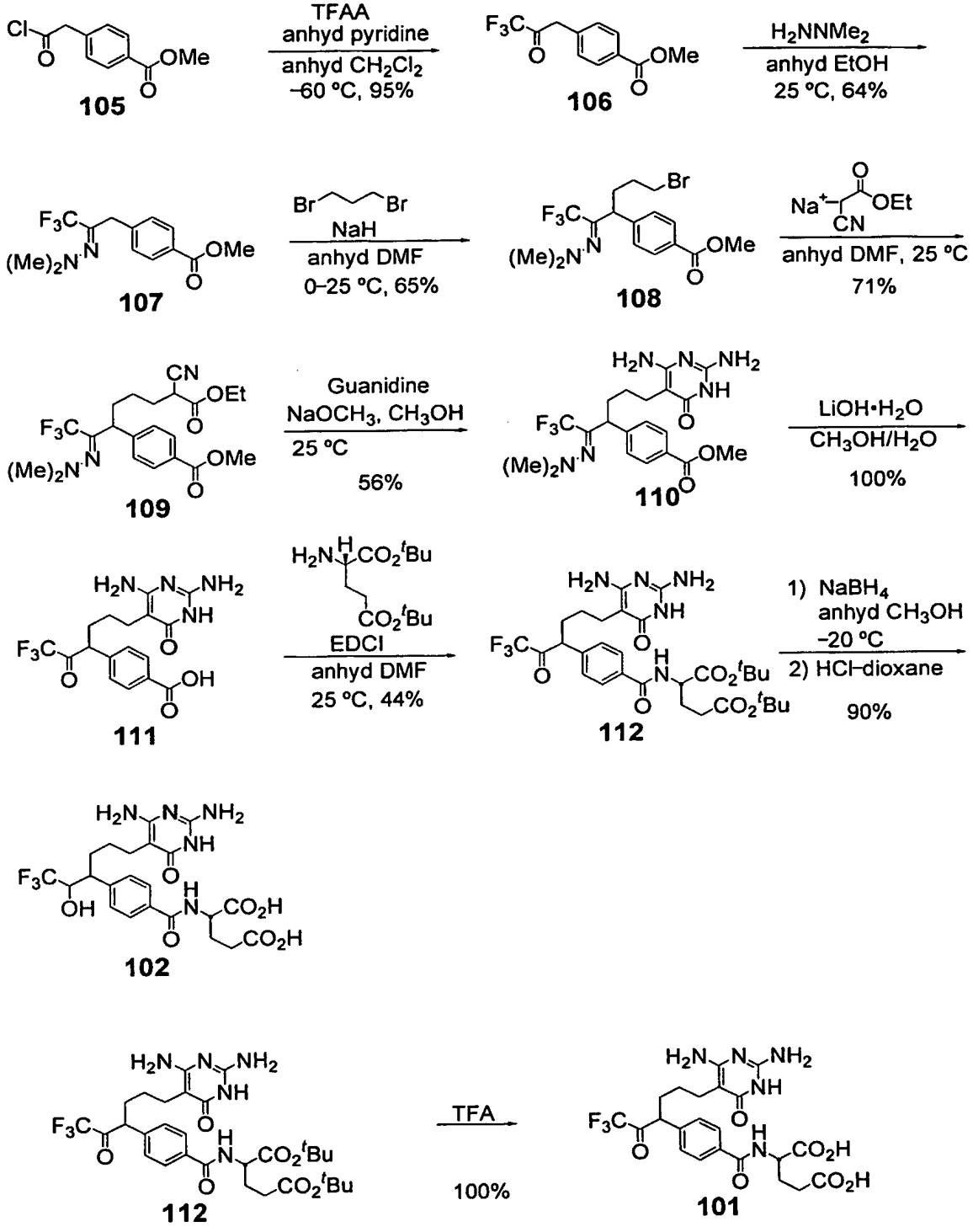
TFAA
anhyd pyridine
anhyd CH_2Cl_2
−60 °C, 95%
H_2NNMe_2
anhyd EtOH
25 °C, 64%
NaH
anhyd DMF
0–25 °C, 65%
anhyd DMF, 25 °C
71%
Guanidine
$NaOCH_3$, CH_3OH
25 °C
56%
$LiOH·H_2O$
CH_3OH/H_2O
100%
EDCI
anhyd DMF
25 °C, 44%
1) $NaBH_4$
anhyd CH_3OH
−20 °C
2) HCl-dioxane
90%
TFA
100%
105
106
107
108
109
110
111
112
102
101

Figure 15

GAR and AICAR Tfase Inhibition (K_i, μM)

Compound	*E.coli* GAR Tfase	rhGAR Tfase	rhAICAR Tfase
10-CF_3CO-DDACTHF (**101**)	1.9	0.015	>100
10-CF_3HCOH-DDACTHF (**102**)	20	0.900	>100
10-formyl-DDACTHF (**3**)	6	0.14	1
DDACTHF	5	1.7	not determined
Lometrexol	0.1	not determined	not determined

Figure 16

In Vitro Cytotoxic Activity

Compound	CCRF-CEM (IC_{50}, μM)			
	(+) T, (+) H	(-) T, (+) H	(+) T, (-) H	(-) T, (-) H
10-CF_3CO-DDACTHF (**101**)	>100	>100	0.017	0.016
10-CF_3HCOH-DDACTHF (**102**)	>100	>100	1.4	1.1
10-formyl-DDACTHF (**3**)	150	170	0.06	0.07
DDACTHF	>100	>100	3.6	2.7
Lometrexol	>100	>100	0.52	0.23
Methotrexate	0.05	0.05	0.04	0.04

T = Thymidine (+ 10 μM), H = Hypoxanthine (+ 100 μM)

Figure 17

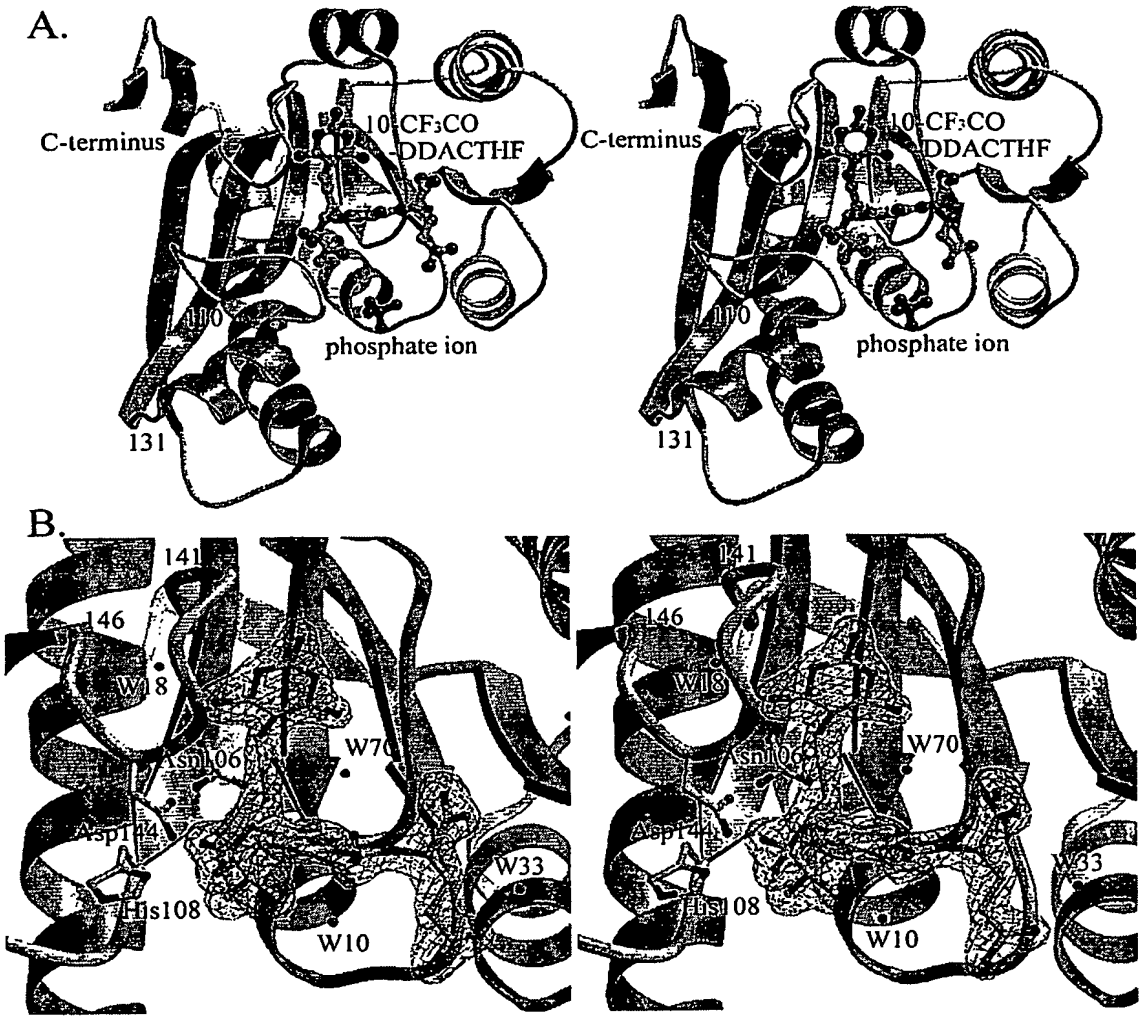
A.
C-terminus
10-CF3CO
-DDACTHF
110
phosphate ion
131
C-terminus
10-CF3CO
DDACTHF
110
phosphate ion
131
B.
141
146
W18
W70
Asn106
Asp144
W33
His108
W10
141
146
W18
W70
Asn106
Asp144
W33
His108
W10

Figure 18

B value comparison of unliganded human GAR Tfase, *E.coli* GAR Tfase in complex with 10-formyl-TDAF and substrate, and human GAR Tfase in complex with 10-CF_3CO-DDACTHF (**101**)

	Human complex with 10-CF_3CO-DDACTHF (**101**)		*E.coli* complex with 10-formyl-TDAF-β-GAR	Unliganded human
	Molecule 1	Molecule 2		
	($Å^2$)	($Å^2$)	($Å^2$)	($Å^2$)
Protein	31.0	35.3	29.6	30.1
Inhibitor	25.8	39.3	43.5	-
Residues 110-131	22.4	26.6	41.1	23.6
Residues 141-146	30.0	37.5	45.4	64.4

Figure 19

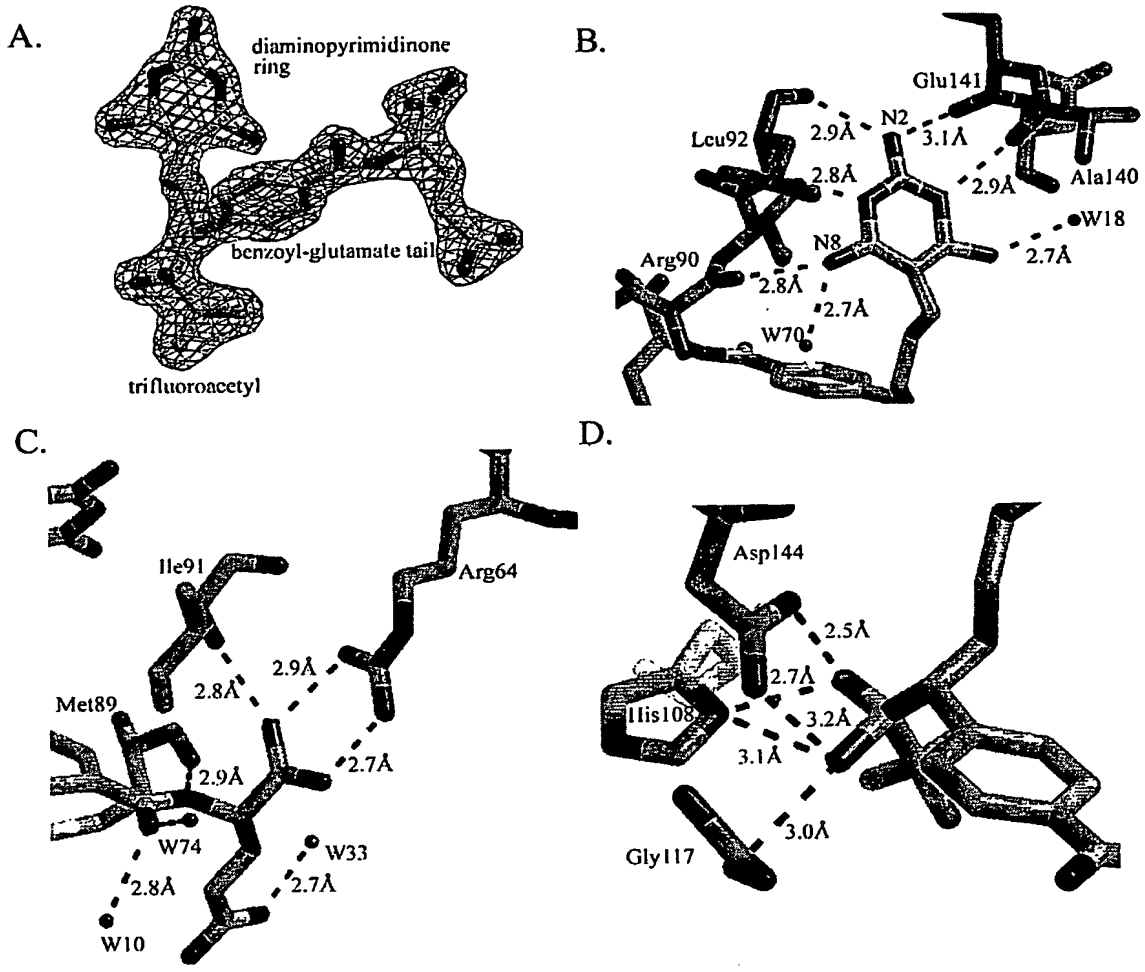
A.
diaminopyrimidinone ring
benzoyl-glutamate tail
trifluoroacetyl
B.
Glu141
Leu92
2.9Å
N2
3.1Å
2.8Å
2.9Å
Ala140
W18
N8
2.7Å
Arg90
2.8Å
2.7Å
W70
C.
Ile91
Arg64
2.8Å
2.9Å
Met89
2.9Å
2.7Å
W74
W33
2.8Å
2.7Å
W10
D.
Asp144
2.5Å
2.7Å
His108
3.2Å
3.1Å
3.0Å
Gly117

Figure 20

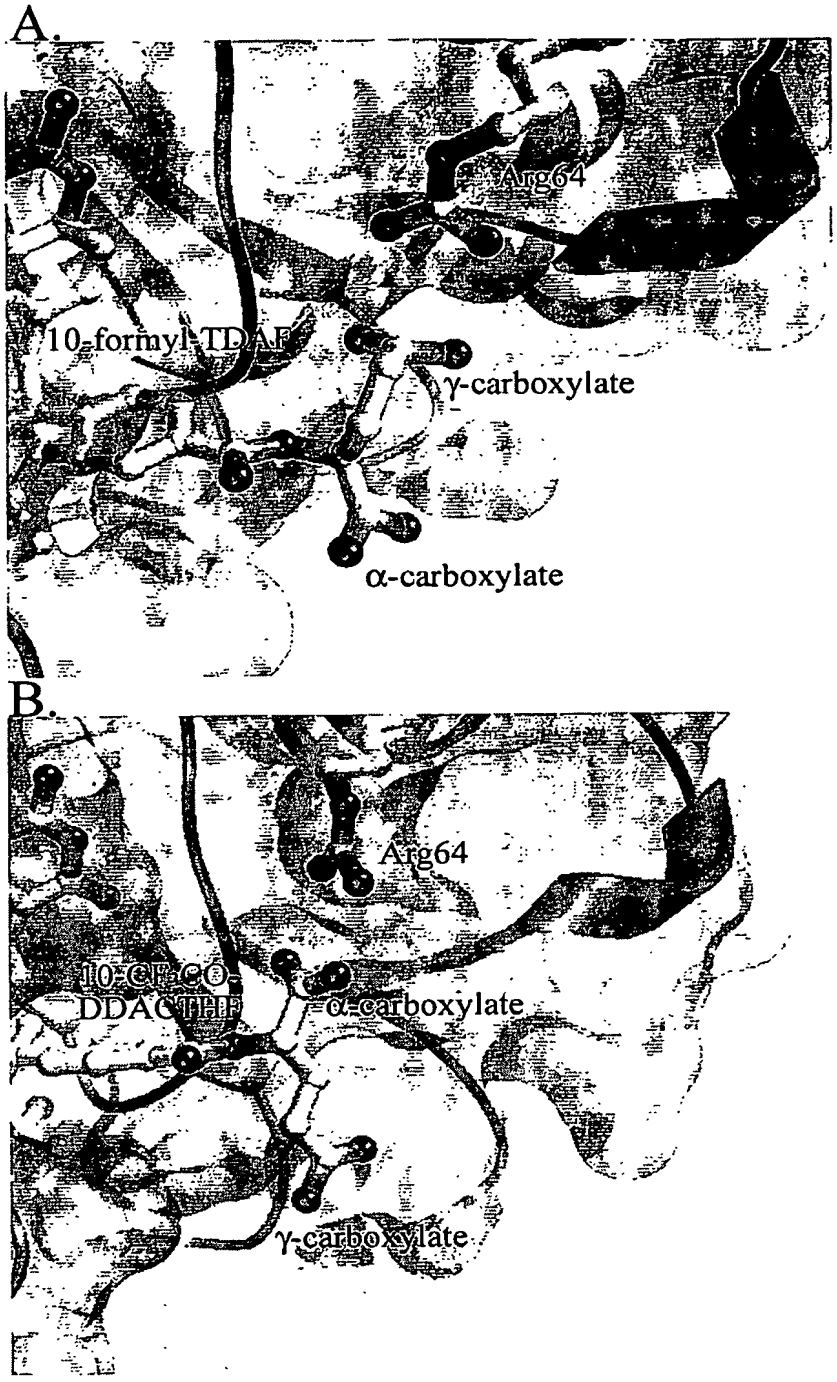
A.
Arg64
10-formyl-TDAF
γ-carboxylate
α-carboxylate
B.
Arg64
10-CF3CO-
DDACTHF
α-carboxylate
γ-carboxylate

Figure 21

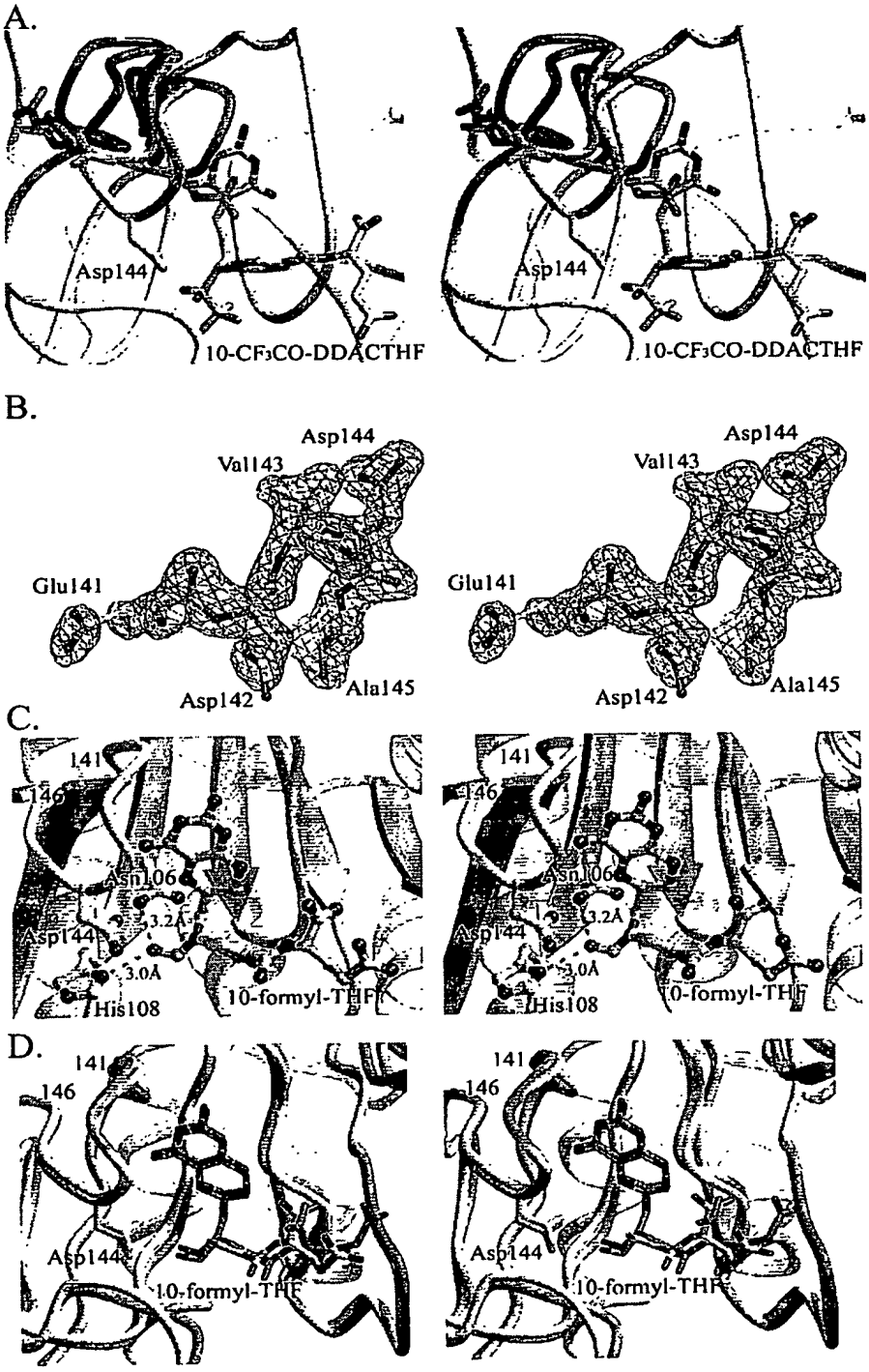
A.
Asp144
10-CF3CO-DDACTHF
Asp144
10-CF3CO-DDACTHF
B.
Asp144
Val143
Glu141
Asp142
Ala145
Asp144
Val143
Glu141
Asp142
Ala145
C.
141
146
Asn106
3.2Å
Asp144
3.0Å
His108
10-formyl-THF
141
146
Asn106
3.2Å
Asp144
3.0Å
His108
10-formyl-THF
D.
141
146
Asp144
10-formyl-THF
141
146
Asp144
10-formyl-THF

Figure 22

Docking of folate cofactor into human and *E.coli* GAR Tfase structures

Structure of PDB code	Number of clusters	Percentage of conformers in the lowest cluster	Docking E (kcal/mol)	Binding E (kcal/mol)
Human recombinant				
101	6	49	-19.0	-15.5
apo (1MEJ)	11	15	-16.4	-13.1
E.coli				
10-Formyl-TDAF + β-GAR (1C2T)	2	38	-17.7	-14.5
BW1476U89 (1GAR)	1	100	-16.9	-13.2
Epoxide + β-GAR (1JKX)	3	68	-15.5	-12.2
apo (1CDE)	18	22	-13.9	-11.0

Figure 23